Modeling and Control of Human Motor System with Generalized Predictive Control

L. Lan
School of Electrical and Electronic Engineering
Nanyang Technological University
Singapore
lanli@pmail.ntu.edu.sg

K.Y. Zhu
School of Electrical and Electronic Engineering
Nanyang Technological University
Singapore
ekyzhu@ntu.edu.sg

D.G. Zhang
School of Electrical and Electronic Engineering
Nanyang Technological University
Singapore
killtears@hotmail.com

***Abstract*— Many patients suffer from the spinal cord diseases, a proper modeling and control of human motor system will help to improve the prognosis of them. This paper presents an integrated model to describe the static and dynamic characters of spinal neuro-musculoskeletal system based on the currently accepted theories and hypothesis in biological motor control. Then a new control system with Generalized Predictive Control and neural network is designed to control the former model.**

***Keywords*—Motor control, Spinal neuro-musculoskeletal system, Generalized Predictive Control, Neural network.**

I. INTRODUCTION

In the cases of spinal cord diseases such as spinal cord trauma, degenerative myelopathy, infectious or inflammatory disease and neoplastic diseases, patient may lose the sense and motor control function. In this study, we intend to develop a control system to get the descending commands for spinal neuro-musculoskeletal system, which will be helpful to improve the prognosis of the patient. Furthermore, this study will also give us good ideas to develop new control algorithms and design advanced control systems which will lead to new insights to industry, such as human-machine interfaces and robotics.

In the central nervous system of human motor system, the spinal cord transmits motor commands and sensory information and generates simple movements. If the spinal cord lost most function, the descending command from higher center to the spinal cord will be blocked. Thus, for rebuilding the motor system of paralyzed patient, we need to build a fairly completed neuro-musculoskeletal system based on experimental data and develop a controller with proper control strategy.

Therefore, in following contents, we first propose an elaborate model for neuro-musculoskeletal system, which contains enough detail in both anatomical structure and dynamic properties to be useful, so the model can simulate experimental observations and generate predictions of interacting modulation of muscle behavior after combing with model for control system. Then, we develop a new controller with Generalized Predictive Control (GPC) and neural network to control the limb active movement.

II. MODELING OF NEURO-MUSCULOSKELETAL SYSTEM

Fig.1 shows the block diagram of neuro-musculoskeletal system, in which, the muscle joint system consists of a pair of antagonists around a hinge joint. The Hill-type model is adopted to describe the dynamics of both flexor and extensor.

For simplicity, in following contents, Subscript f and e represent the characters for flexor and extensor muscles. Superscript M represents muscle, T represents tendon, and MT represents the musculo-tendon system.

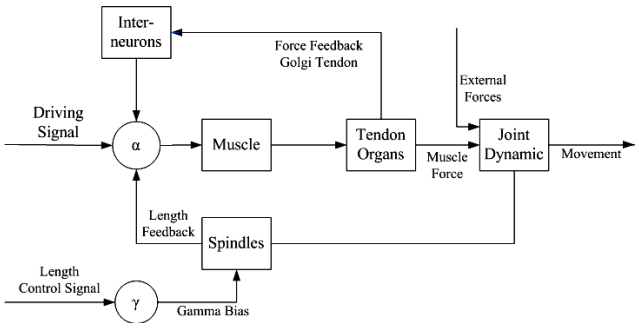

Figure 1. The block diagram of spinal neuro-musculoskeletal system. Inputs to α -motoneurons cause muscles to produce force which shortens muscles and changes joint angles. Spindle afferents detect changes in muscle-length, and biased by activity in the γ-motoneurons. The golgi tendon organs detect tension,and send the signal to inhibitory interneurons.

1-4244-0025-2/06/$20.00 ©2006 IEEE

A. Muscle Activation

Based on the Equilibrium Point Hypothesis of human motor system, we assume that the nervous system may coordinate changes in flexor threshold angles (λ_f) and extensor threshold angles (λ_e), which is determined by the reciprocal (R) and coactivation (C) commands. The dynamic threshold (λ_f^*, λ_e^*) depend on the static ones and angular velocity ($\omega = d\theta/dt$) [1]:

$$\lambda_f = R - C,\ \lambda_e = R + C$$
$$\lambda_f^* = \lambda_f - \mu\omega,\ \lambda_e^* = \lambda_e - \mu\omega \quad (1)$$

where μ is a damping factor [1]. Thus, we assume that motoneuron pool background activation c_f and c_e can be calculated by experimental equations, where $[x]^+=x$ if $x\geq 0$ and $[x]^+=0$ if $x<0$:

$$c_f = e^{\alpha[\theta-\lambda_f^*]^+} - 1, c_e = e^{\alpha[\lambda_e^*-\theta]^+} - 1 \quad (2)$$

The motoneuron pool outputs are determined by both the background activation and the contribution of stretch reflex, reciprocal inhibition and recurrent inhibition. The output of motoneuron pool is modeled as the sum of all excitatory (positive) and inhibitory (negative) inputs, and is given as [2]:

$$u_f(t) = c_f(t)\frac{1}{1+c_f(t)g_f}(1 + s_f v_f - r_f v_e - I_f^{GTO})$$
$$u_e(t) = c_e(t)\frac{1}{1+c_e(t)g_e}(1 + s_e v_e - r_e v_e - I_e^{GTO}) \quad (3)$$

where $u_f(t)$ and $u_e(t)$ represent the output of motoneuron pools for flexor and extensor muscles, that is, the neural input signal. s_f, s_e are stretch reflex gains; r_f, r_e are reciprocal inhibition gains; g_f, g_e are Renshaw cell gains and v_f, v_e are proportional to Ia afferent discharge frequencies of spindles from the flexor and extensor (see spindle dynamics), I_f^{GTO} and I_e^{GTO} are the feedback of Golgi tendon organs.

Based on Zajac's previous work [3], the dynamics of muscle activation $a(t)$ is determined by the neural input signal $u(t)$, the relationship is described as follows:

$$\frac{da_f(t)}{dx} = -\frac{1}{\tau_f}a_f(t) + \frac{1}{\tau_f}u_f(t)$$
$$\frac{da_e(t)}{dx} = -\frac{1}{\tau_e}a_e(t) + \frac{1}{\tau_e}u_e(t) \quad (4)$$

where τ_f, τ_e are time constants for the muscle activation of flexor and extensor, respectively.

B. Muscle Mechanical Properties

The muscle mechanical properties describe the general structure and physical characters of the muscle, which include the muscle active force, muscle passive force and tendon interacts.

1) Active force:

The muscle model follows a general hill-type model. Active muscle force is defined as the product of force-length, and force-velocity factors with muscle activation

$$F^M = F_0^M \widetilde{FL}(\tilde{L}^M)\widetilde{FV}(\tilde{V}^M)a(t) \quad (5)$$

where $\tilde{L}^M$ represents the muscle length normalized to optimal muscle fiber length(L_0^M), $\tilde{V}^M$ is the muscle contraction velocity normalized to its maximal shorting velocity(V_0^M). $\widetilde{FL}(L)$ describes how the normalized active force output of muscle is dependent on its length L. $\widetilde{FV}(V)$ describes how the normalized active force is depend on its speed V. $a(t)$ is the muscle activation. F_0^M is the maximal isometric force.

Based on the former work of Zajac, $\widetilde{FV}(V)$ is given as:

$$\widetilde{FV}(V) = \frac{a}{1+e^{b(\tilde{V}^M - c)}} \quad (6)$$

$\widetilde{FL}(L)$ is given as follows:

$$\widetilde{FL}(L) = d(\tilde{L}^M)^2 - 2d\tilde{L}^M + d + 1 \quad (7)$$

where a, b, c, d are constants.

2) Passive force

Passive forces provide a virtually immediate influence that promotes limb stability. Kirsch et al. [4] found that the passive muscle stiffness and viscosity estimates depended on the statistical properties of the perturbations. The e passive muscle force is given as following equations:

$$F_P = f_P(l) + B_P(l)\cdot v \quad (8)$$

$$f_P(l) = \begin{cases} 0.1663\{\exp[208.2(l-0.036)]-1\} & 0.036 < l < 0.057 \\ 13.0076 + 2743(l-0.057) & l \geq 0.057 \\ 0 & l \leq 0.036 \end{cases} \quad (9)$$

$$B_P(l) = \begin{cases} 0.34624\{\exp[208.2(l-0.036)]\} & l < 0.057 \\ 27.4 & l \geq 0.057 \end{cases} \quad (10)$$

In these equations, the muscle velocity v and length l are normalized by the maximum speed of shortening and the optimal fiber length, respectively.

3) Tendon Interacts

The dynamic properties of muscle-tendon can be expressed by a first-order differential equation [5]:

$$\frac{d\tilde{F}^{MT}}{dt} = \tilde{K}^T(\tilde{V}^{MT} - \tilde{V}^M) \quad (11)$$

where $\tilde{F}^{MT}$ represents normalized muscle-tendon force, it equal to normalized muscle force and normalized tendon force ($\tilde{F}^{MT} = \tilde{F}^M = \tilde{F}^T$); $\tilde{V}^{MT}$ represents normalized muscle-tendon velocity; $\tilde{V}^M$ represents normalized muscle velocity; t represents time; and $\tilde{K}^T$ represents normalized tendon stiffness.

We modeled the tendon as a linear spring, with a stiffness of K^T. Because the tendon force was the same as muscle force, thus, tendon length could be determined as [5]:

$$L^T = \frac{F^M}{K^T} + L^{TS} \tag{12}$$

where L^{TS} is the tendon slack length, which is determined as in:

$$L^{TS} = L_0^{MT} - 1.2L_0^M \tag{13}$$

where L_0^{MT} is the maximally elongated musculo-tendon length.

Thus muscle length could be obtained from the musculo-tendon length by following equation [5]:

$$L^M = L^{MT} - L^T \tag{14}$$

Coupled with Eq. (12) we have:.

$$L^M = L^{MT} - \frac{F^M}{K^T} - L^{TS} \tag{15}$$

C. Joint Dynamics

The joint torque T_j is calculated as follows:

$$T_j = F_f \cdot h_f - F_e \cdot h_e + T_L \tag{16}$$

where F_f and F_e are forces of flexor and extensor; T_L is an external torque applied to the joint.

The dynamic properties of a joint are calculated as follows:

$$I_j \frac{d^2\theta}{dt^2} + B_j \frac{d\theta}{dt} = T_j \tag{17}$$

$$\kappa = K_f + K_e = K_f^M \cdot h_f^2 + K_e^M \cdot h_e^2 \tag{18}$$

$$B_j = 0.03\kappa \tag{19}$$

where I_j is the moment of inertia; B_j is the coefficient of viscosity; θ is the joint angle; κ is joint stiffness; K_f and K_e are joint stiffness of flexor and extensor muscles; while K_f^M and K_e^M are muscle stiffness of flexor and extensor, respectively. Passive elastic joint force is ignored. Joint viscosity is also related to muscle active stiffness by (18) [6].

The relation in (19) is given in [7]. Muscle active stiffness for flexor and extensor is defined under isometric condition as follows:

$$\begin{aligned} K_f^M &= \frac{\partial F_f}{\partial L_f^M} = \frac{F_{of}^M}{L_{of}^M} \cdot a_f(t) \cdot d \cdot 2 \cdot (\tilde{L}_f^M - 1) \\ K_e^M &= \frac{\partial F_e}{\partial L_e^M} = \frac{F_{oe}^M}{L_{oe}^M} \cdot a_e(t) \cdot d \cdot 2 \cdot (\tilde{L}_e^M - 1) \end{aligned} \tag{20}$$

where F_{of}^M, F_{oe}^M, L_{of}^M and L_{oe}^M are maximal isometric muscle force and optimal fiber length for flexor and extensor muscles.

D. Muscle receptors

Muscle receptors monitor the statement of the moving elements, and transfer the feed back signal to the motor neuron in spinal cord, which mainly includes the muscle spindle and Golgi Tendon orgons.

1) Golgi Tendon Organs

In this study, we used the model of Houk and Simon to describe the dynamics of the Golgi tendon organ response to muscle force. The applicability of this model to tendon organ afferent behavior during normal motion was confirmed by Prochazka and Gorassini [8,9].

The transfer function for Golgi tendon organ is a band-pass filter [9]:

$$H_{GTO}(S) = K_{GTO} \frac{(1+\frac{S}{0.15})(1+\frac{S}{1.5})(1+\frac{S}{16})}{(1+\frac{S}{0.2})(1+\frac{S}{2})(1+\frac{S}{37})} \tag{21}$$

2) Spindle Dynamics

In this report, we assume a lumped, linear dynamics of a spring-damper model of spindle to provide muscle length and velocity feedback [10]. The dynamics of the spindle is given by

$$T_S(1+\frac{K_{PE}}{K_{SE}}) + \frac{B_S}{K_{SE}} \cdot \frac{dT_S}{dt} = B_S \frac{dx}{dt} + K_{PE}x + T_{S0}(\gamma) \tag{22}$$

where T_S is the tension within the spindle, x is spindle length, we assume it is equal to the muscle length in this study, K_{SE} and K_{PE} are serial and parallel stiffness of the spindle, and B_S is the damping coefficient of the spindle, $T_{S0}(\gamma)$ is the tension generated by spindle, which is assumed to be proportional to the intensity of activation [2], that is:

$$T_{S0}(\gamma) = P\gamma,$$

where γ is the fusimotor input to the spindle, and P is a constant.

In fact, we need two fusimotor inputs to the spindles in flexor muscle and extensor, respectively. However, Neurophysiological evidence [11,12] suggests that single cortico-motoneurons can activate premotor interneurons in the spinal cord that exhibits reciprocal control of antagonist muscles through fusimotor-activated spindle afferents. Therefore, it is possible for using a single static command to govern the spindles of both flexor and extensor muscles in a differential manner via a proper bias by spinal interneuronal network [2].

For convenience, we define the range of the descending drive parameter as $-0.5 \le \gamma \le 0.5$. For flexor and extensor spindles, their static inputs are given as [2]:

$$\gamma_f = 0.5 + \gamma, \ \gamma_e = 0.5 - \gamma \tag{23}$$

where γ_f and γ_e are the static fusimotor input to the flexor and extensor spindles, respectively.

The output signal to motoneuron is proportional to the tension within the fusimotor fiber, such as [2]:

$$\upsilon = \frac{A \bullet T_S}{K_{SE}},$$

where A is a constant.

III. DESIGN OF CONTROL SYSTEM

A. Process Description

Consider the nonlinear musculoskeletal system described by the following discrete-time model

$$y(t) = f_p[y(t-1),\cdots,y(t-n_y); \quad (24)$$
$$u(t-1),\cdots,u(t-n_u)] + \xi(t)$$

where $y(t), u(t)$ are system output and input. $\{\xi(t)\}$ is the random sequence. It is assumed that nonlinear model can be generally described by the following locally-linearized and discrete-time model [13,14]:

$$A(z^{-1})y(t) = B(z^{-1})u(t-1) + N(t-1) + \xi(t) \quad (25)$$

where $A(z^{-1}), B(z^{-1})$ are diagonal polynomial matrices in the backforward shift operator z^{-1} with $n_A < n_y, n_B < n_u$,

$$A(z^{-1}) = I + A_1 z^{-1} + \cdots + A_{n_A} z^{-n_A}$$

$$B(z^{-1}) = B_0 + B_1 z^{-1} + \cdots + B_{n_B} z^{-n_B}$$

$N(t)$ denotes the model error including the unmodelled dynamics, nonlinearity of the system, which will be identified on-line by the neural network in the future work. We will consider $N(t)$ in the design of the GPC control strategy, but in the following simulations and calculations, we will only consider the linear component.

In equation (25), $N(t-1) + \xi(t)$ can be considered as [13]:

$$N(t-1) + \xi(t) = C(z^{-1})\xi'(t)/\Delta \quad (26)$$

where $C(z^{-1}) = 1 + c_1 z^{-1} + \cdots + c_{nc} z^{-n_c}$, Δ is the differencing operator $1 - z^{-1}$, and $\xi'(t)$ is an uncorrelated random sequence. Combining with equation (25), we obtain the CARIMA (Control Auto-Regressive and Integrated Moving-Average) model:

$$A(z^{-1})y(t) = B(z^{-1})u(t-1) + C(z^{-1})\xi'(t)/\Delta \quad (27)$$

This simplicity is the most cases, which occur in the control system design. However, in our design, we will take into account the nonlinearity component so that its influence can be effectively reduced.

B. Output Predictor

To build a j-step ahead predictor of $y(t+j)$, consider the following diophantine equation:

$$1 = E_j(z^{-1})A(z^{-1}) + z^{-j}F_j(z^{-1}) \quad (28)$$

where $E_j(z^{-1})$ and $F_j(z^{-1})$ are polynomials uniquely determined by $A(z^{-1})$ and j.

$$E_j(z^{-1}) = 1 + e_1 z^{-1} + \cdots + e_{j-1} z^{-j+1}$$

$$F_j(z^{-1}) = f_{j0} + f_{j1} z^{-1} + \cdots + f_{j,n_a-1} z^{-n_a+1}$$

Premultiply equation (25) by $E_j(z^{-1})$ and use equation (28), we have

$$y(t+j) = E_j(z^{-1})B(z^{-1})u(t+j-(t+j-1)) \quad (29)$$
$$+ F_j(z^{-1})y(t) + E_j(z^{-1})\xi(t+j)$$

As $E_j(z^{-1})$ is of degree $j-1$, $E_j(z^{-1})\xi(t+j)$ is uncorrelated with other terms so that the optimal predictor, given measured output data up to time t and any $u(t+i), N(t+i)$ for $i > 1$, is clearly:

$$\hat{y}(t+j/t) = E_j(z^{-1})B(z^{-1})u(t+j-1) \quad (30)$$
$$+ E_j(z^{-1})N(t+j-1) + F_j(z^{-1})y(t)$$

$$\hat{y}(t+j/t) = y(t+j) - E_j(z^{-1})\xi(t+j) \quad (31)$$

In equation (30), $\hat{y}(t+j/t)$ is a function of known signal values at time t and also of future control inputs which have yet to be computed. A second Diophantine equation may now be introduced to break up $E_j(z^{-1})B(z^{-1})$ into two parts and distinguish between past and future control values.

$$E_j(z^{-1})B(z^{-1}) = G_j(z^{-1}) + z^{-j}L_j(z^{-1}) \quad (32)$$

where $G_j(z^{-1})$ and $L_j(z^{-1})$ are polynomials.

$$G_j(z^{-1}) = g_0 + g_1 z^{-1} + \cdots + g_{j-1} z^{-j+1}$$

$$L_j(z^{-1}) = l_{j0} + l_{j1} z^{-1} + \cdots + l_{j,n_b-1} z^{-n_b+1}$$

Then the output prediction is given by:

$$\hat{y}(t+j/t) = G_j(z^{-1})u(t+j-1) + E_j(z^{-1})N(t+j-1) \quad (33)$$
$$+ F_j(z^{-1})y(t) + L_j(z^{-1})u(t-1)$$

C. Cost Function of GPC

Consider the following quadratic cost function:

$$J(N_p) = E\{\sum_{j=1}^{N_p}[y(t+j) - r_j w(t+j) + H_j(z^{-1})N(t+j-1)]^2 \quad (34)$$
$$+ \sum_{j=1}^{N_p}\lambda_j u(t+j-1)^2\}$$

where N_p is the prediction horizon. $w(t)$ is reference signal. r_j, λ_j are constant weights. $H_j(z^{-1})$ is a polynomial, whose role is to reduce the effect of $N(t)$ on the closed-loop system, so that the control performance can be improved.

D. Controller Design

1) Control law of GPC

A set of the output predictors is given by:

$$\hat{y}(t+1/t) = G_1 u(t) + E_1 N(t) + F_1 y(t) + L_1 u(t-1)$$
$$\hat{y}(t+2/t) = G_2 u(t+1) + E_2 N(t+1) + F_2 y(t) + L_2 u(t-1)$$
$$\vdots$$
$$\hat{y}(t+N_p/t) = G_{N_p} u(t+N_p-1) + E_{N_p} N(t+N_p-1)$$
$$+ F_{N_p} y(t) + L_{N_p} u(t-1)$$

The above equations can be written in the matrix form:

$$Y = GU + EN + Fy(t) + Lu(t-1) \quad (35)$$

where

$$Y=\begin{bmatrix}\hat{y}(t+1/t)\\ \hat{y}(t+2/t)\\ \vdots\\ \hat{y}(t+N_p/t)\end{bmatrix}\qquad U=\begin{bmatrix}u(t)\\ u(t+1)\\ \vdots\\ u(t+N_p-1)\end{bmatrix}$$

$$N=\begin{bmatrix}N(t)\\ N(t+1)\\ \vdots\\ N(t+N_p-1)\end{bmatrix}\quad G=\begin{bmatrix}g_0 & & 0\\ g_1 & g_0 & \\ \vdots & & \ddots\\ g_{N_p-1} & g_{N_p-2} & \cdots & g_0\end{bmatrix}$$

$$E=diag[E_j(z^{-1})]=\begin{bmatrix}E_1(z^{-1}) & & 0\\ & E_2(z^{-1}) & \\ & & \ddots\\ 0 & & E_{N_p}(z^{-1})\end{bmatrix}$$

$$F=\begin{bmatrix}F_1(z^{-1})\\ F_2(z^{-1})\\ \vdots\\ F_{N_p}(z^{-1})\end{bmatrix}\qquad L=\begin{bmatrix}L_1(z^{-1})\\ L_2(z^{-1})\\ \vdots\\ L_{N_p}(z^{-1})\end{bmatrix}$$

From the above definitions and with

$$W=\begin{bmatrix}w(t+1)\\ w(t+2)\\ \vdots\\ w(t+N_p)\end{bmatrix}\qquad R=diag(r_j)\qquad \lambda=diag(\lambda_j)$$

$$H=diag[H_j(z^{-1})]\ \ (j=1,2,\cdots,N_p)$$

Equation (34) becomes:

$$\begin{aligned}J(N_p)&=E\{(Y-RW+HN)^T(Y-RW+HN)+U^T\lambda U\}\\&=E\{\|Y-RW+HN\|_I^2+\|U\|_\lambda^2\}\\&=E\{\|GU+(E+H)N+Fy(t)+Lu(t-1)-RW\|_I^2+\|U\|_\lambda^2\}\end{aligned}$$

where $\|x\|_Q^2=x^TQx$. Optimizing $J(N_p)$ with respect to U, we obtain

$$U=(G^TG+\lambda)^{-1}G^T[RW-Fy(t)-Lu(t-1)-(E+H)N] \tag{36}$$

Using the receding horizon control philosophy, only the first element $u(t)$ is actually implemented. That is, only the top row of U needs to be computed.

Define $[\alpha_1,\alpha_2,\cdots,\alpha_{N_p}]$ to be the first row of $(G^TG+\lambda)^{-1}G^T$, then

$$u(t)=[\alpha_1,\alpha_2,\cdots,\alpha_{N_p}][RW-Fy(t)-Lu(t-1)-(E+H)N] \tag{37}$$

2) Closed-loop System

Equation (37) becomes:

$$\{1+z^{-1}[\alpha_1,\alpha_2,\cdots,\alpha_{N_p}]L\}u(t)=[\alpha_1,\alpha_2,\cdots,\alpha_{N_p}][RW-Fy(t)-(E+H)N]$$

Then

$$\begin{aligned}[1+z^{-1}\sum_{i=1}^{N_p}\alpha_iL_i(z^{-1})]u(t)&=(\sum_{i=1}^{N_p}\alpha_ir_iz^i)w(t)-\\&[\sum_{i=1}^{N_p}\alpha_iF_i(z^{-1})]y(t)-\{\sum_{i=1}^{N_p}\alpha_i[E_i(z^{-1})+H_i(z^{-1})]z^{i-1}\}N(t)\end{aligned} \tag{38}$$

Premultiplying equation (25) by $[1+z^{-1}\sum_{i=1}^{N_p}\alpha_iL_i(z^{-1})]$, and using (38), we obtain the closed-loop system:

$$\begin{aligned}&[A(1+z^{-1}\sum_{i=1}^{N_p}\alpha_iL_i)+z^{-1}B\sum_{i=1}^{N_p}\alpha_iF_i]y(t)=B(\sum_{i=1}^{N_p}\alpha_ir_iz^{i-1})w(t)\\&+z^{-1}[1+z^{-1}\sum_{i=1}^{N_p}\alpha_iL_i-B\sum_{i=1}^{N_p}\alpha_i(E_i+H_i)z^{i-1}]N(t)\\&+(1+z^{-1}\sum_{i=1}^{N_p}\alpha_iL_i)\xi(t)\end{aligned} \tag{39}$$

3) Reduction of nonlinearity influence

To reduce the influence of nonlinearities in the closed-loop system, the term containing $N(t)$ should be as small as possible. In ideal case, it should be

$$z^{-1}[1+z^{-1}\sum_{i=1}^{N_p}\alpha_iL_i-B\sum_{i=1}^{N_p}\alpha_i(E_i+H_i)z^{i-1}]N(t)=0$$

That means

$$B\sum_{i=1}^{N_p}\alpha_i(E_i+H_i)z^{i-1}=1+z^{-1}\sum_{i=1}^{N_p}\alpha_iL_i \tag{40}$$

Premultiplying (37) by $B(z^{-1})$ and using (40) result in:

$$\begin{aligned}Bu(t)=B[\alpha_1,\alpha_2,\cdots,\alpha_{N_p}][RW-Fy(t)-Lu(t-1)]\\-(1+z^{-1}\sum_{i=1}^{N_p}\alpha_iL_i)N(t)\end{aligned}$$

Clearly, if $B(z^{-1})$ is stable and invertible, then

$$\begin{aligned}u(t)=[\alpha_1,\alpha_2,\cdots,\alpha_{N_p}][RW-Fy(t)-Lu(t-1)]\\-B^{-1}(1+z^{-1}\sum_{i=1}^{N_p}\alpha_iL_i)N(t)\end{aligned} \tag{41}$$

Assuming $r_1=r_2=\cdots=r_{N_p}=r$, then $R=rI$. From equation (39), r should be chosen as

$$r=(\sum_{i=1}^{N_p}\alpha_i)^{-1}\{B(1)^{-1}A(1)[1+\sum_{i=1}^{N_p}\alpha_iL_i(1)]+\sum_{i=1}^{N_p}\alpha_iF_i(1)\} \tag{42}$$

E. Neural Network Identifier

Note that in (41) $N(t)$ is unknown, which will be identified on-line by a BP (backpropagation) net with 3 layers in the algorithm. Its structure is given in Fig.2. There are s units in the input layer, m sigmoidal neurons in the hidden layer and n linear neurons in the output layer. w_{jp},β_j are the corresponding weights and thresholds between input and hidden layer, while w_{ij},β_i are those between hidden and output layer, for $p=1,\cdots,s;\ j=1,\cdots,m;i=1,\cdots,n$.

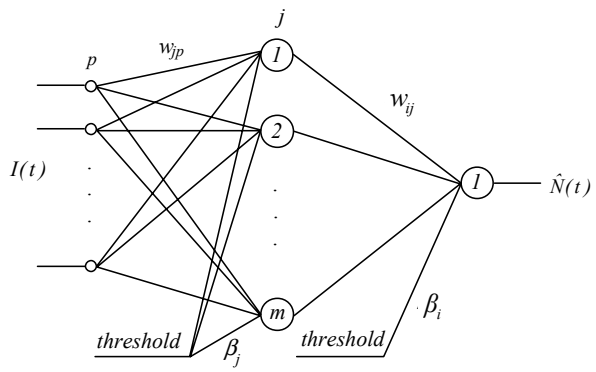

Figure 2. BP net structure (where n=1)

The network input vector is

$$I(t) = [y(t)^T, y(t-1)^T, \cdots; u(t-1)^T, u(t-2)^T, \cdots; \\ y^*(t)^T, y^*(t-1)^T, \cdots]^T \quad (43)$$

where, taking the *ith* input-output path into account $(i = 1,2,\cdots,n)$,

$$y_i^*(t) = [1 - A^i(z^{-1})]y_i(t) + B^i(z^{-1})u_i(t-1) \quad (44)$$
$$= -a_1^i y_i(t-1) - \cdots - a_{n_{a^i}}^i y_i(t-n_{a^i}) \\ + b_0^i u_i(t-1) + \cdots + b_{n_{b^i}}^i u_i(t-n_{b^i})$$

The teaching signal is

$$d_i(t-1) = y_i(t) - y_i^*(t) \quad (45)$$

The weights and thresholds are updated using fast BP algorithm, which is improved by techniques of momentum and an adaptive learning rate to increase the training speed and reliability. Then the final output $\hat{N}(t)$ can be obtained, which is the estimate of $N(t)$.

IV. Conclusion

This short paper presented a fairly completed model of spinal neuro-musculoskeletal system in the human motor system and a new control system with Generalized Predictive Control and neural network was designed to control the spinal neuro-musculoskeletal system. The objective of this study is to give an artificial control system for paralyzed patient. Some simulative and clinical experiment will be done in future.

Appendix (Anatomical Arrangement)

The anatomical arrangement of flexor and extensor at the elbow joint is shown in Fig. 3, in which the moment arm of the flexor and extensor are h_f and h_e, the lengths of musculo-tendon are L_f^{MT} and L_e^{MT}, and the velocities are V_f^{MT} and V_e^{MT}. The relations among them can be expressed by the physiological parameters of the elbow joint.

$$h_f = \frac{lplf}{\sqrt{1+\left(\frac{lplf + lpf\cdot\cos\theta}{lpf\cdot\sin\theta}\right)^2}} \quad (1)$$

$$h_e = \frac{lple}{\sqrt{1+\left(\frac{lple - lpe\cdot\cos\theta}{lpe\cdot\sin\theta}\right)^2}} \quad (2)$$

$$L_f^{MT} = \sqrt{lplf^2 + lpf^2 + 2lplf\cdot lpf\cdot\cos\theta} \quad (3)$$

$$L_e^{MT} = \sqrt{lple^2 + lpe^2 - 2lple\cdot lpe\cdot\cos\theta} \quad (4)$$

$$V_f^{MT} = \frac{dL_f^{MT}}{dt} = \frac{-\frac{d\theta}{dt}\cdot lplf\cdot lpf\cdot\sin\theta}{\sqrt{lplf^2 + lpf^2 + 2lplf\cdot lpf\cdot\cos\theta}} \quad (5)$$

$$V_e^{MT} = \frac{dL_e^{MT}}{dt} = \frac{-\frac{d\theta}{dt}\cdot lple\cdot lpe\cdot\sin\theta}{\sqrt{lple^2 + lpe^2 - 2lple\cdot lpe\cdot\cos\theta}} \quad (6)$$

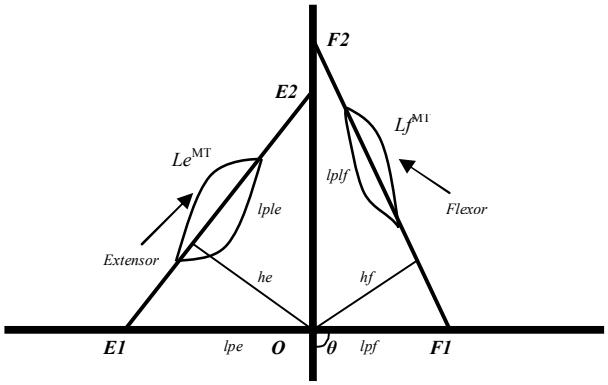

Figure 3. shows the geometric relations between muscle-tendon variables and the joint angle. Point *O* represents the origin of the elbow joint. *F2* and *F1* are the origin and insertion points of the flexor muscle; and *E2* and *E1* are origin and insertion points of the extensor muscle. θ is the elbow joint angle, with 0^o corresponding to full extension, and 180^o to full flexion. Counterclockwise rotation, i.e., flexion, is defined as positive.

These geometric relations are incorporated into the equations of the model for integration of numerical solutions.

References

[1] Feldman, A.G., et al., "The origin of electromyograms – Explanations based on the equilbrium point hypothesis, in Multiple Muscle Systems: Biomechanics and Movement Organization", J. Winters and S.L.-Y. Woo, Springer-Verlag New York Inc.: New York, NY. pp. 195-213. 1990.

[2] N Lan, Y Li, Y Sun, FS Yang, "Reflex regulation of antagonist muscles for control of joint equilibrium position". IEEE Transactions on Neural Systems and Rehabilitation. vol 13, NO. 1, pp. 60-71, 2005.

[3] Zajac, F.E. "Muscle and tendon: properties, models scaling and application to biomechanics and motor control". CRC Critic. Rev. in Biomed. Engng. vol 17, pp. 359-411, 1989.

[4] R. Kirsch, D. Boskov, and W. Rymer, "Muscle stiffness during transient and continuous movements of cat muscle: Perturbation characteristics and physiological relevance," IEEE Trans. Biomed. Eng., vol. 41, pp. 758-770, 1994.

[5] N. Lan, "Stability analysis for posture control in a two joint limb system". IEEE Trans. Neural Syst. Rehab. Eng., vol. 10, no. 4, pp.249–259, 2002.

[6] S. C. Cannon and G. I. Zahalak, “The mechanical behavior of active human skeletal muscle in small oscillations”, J. Biomech., vol. 15, pp. 111–121, 1982.

[7] T. Flash and F. Mussa-Ivaldi, “Human arm stiffness characteristics during the maintenance of posture”. Exp Brain Res. vol. 832, pp. 315–326, 1990.

[8] A. Prochazka and M. Gorassini, “Ensemble firing of muscle spindle afferents recorded during normal locomotion in cats”. J. Physiol., vol. 507, pp.293-304, 1998.

[9] Jiping He, Mitchell G. Maltenfort, Qingjun Wang, and Thomas M. Hamm. “Learning from biological systems: modeling neural control”. IEEE Control Systems Magazine, vol. 21, no.4, pp.55-69.2001.

[10] T. A. McMahon. “Muscles, Reflexes, and Locomotion”. Princeton Univ. Press, pp. 139–167, 1984.

[11] B. A. Lavoie, H. Devanne, and C. Capaday, “Differential control of reciprocal inhibition during walking verus postural and voluntary motor tasks in humans”. J. Neurophysiol., vol. 78, pp. 429–438, 1997.

[12] S. I. Perlmutter, M. A. Maier, and B. E. Fetz, “Activity of spinal interneurons and their effects on forearm muscles during voluntary wrist movements in the monkey”. J. Neurophysiol., vol. 80, pp. 2475–2494, 1998.

[13] D W Clarke, C Mohtadi, and P S Tuffs. “Generalized predictive control—Part I. The basic algorithm. Automatica (Journal of IFAC)”, vol.23 no.2, pp.137-148. 1987.

[14] K Zhu, X Qin, T Chai. “A new decoupling design of self‐tuning multivariable generalized predictive control”. Journal of Adaptive Control and Signal Processing, Vol. 13, No. 2, 183-196.1999.